

Electrocatalytic Degradation of Crystal Violet by a Lead Dioxide Electrode: Operation Parameters and Degradation Mechanism

Yong Guo^{*}, Jun Zong, Anran Gao, Naichuan Yu^{*}

Tianjin Vocational Institute, School of Biological and Environmental Engineering, Tianjin 300410, Peoples R China

*E-mail: 11372662@qq.com(Y. Guo), yunaichuan1119@163.com (N. Yu)

Received: 25 January 2022/ Accepted: 16 March 2022/ Published: 5 April 2022

To explore the treatment methods for crystal violet-containing wastewater, the effects of the initial concentration of crystal violet, current density, electrolyte concentration and pH value on the degradation of crystal violet are studied. The PbO₂ electrode has a good degradation effect on wastewater with different concentrations of crystal violet, especially on those with low concentrations of crystal violet. According to the study, the optimum test conditions for the treatment of crystal violet-containing wastewater with the PbO₂ electrode are finally determined: an initial concentration of crystal violet of 50 mg/L, a current density of 55 mA/cm², a pH value of 4, and an electrolyte concentration of Na₂SO₄ of 0.2 mol/L. The mechanism of crystal violet catalytic oxidation is proposed by analyzing the intermediate products of crystal violet produced from the degradation reaction catalyzed by the lead dioxide electrode. In the process of treating real wastewater containing crystal violet, the highest chemical oxygen demand (COD) removal rate is close to 89% after 6 h of electrolytic treatment, which is a good result, further verifying the degradation performance of the PbO₂ electrode on crystal violet and providing a theoretical basis and practical experience for the technology of treating crystal violet pollutants in the environment.

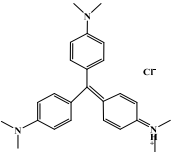
Keywords: Electrochemical degradation, Lead dioxide electrode, Crystal violet, Degradation mechanism

1. INTRODUCTION

Crystal violet (CV) is an excellent dye that is a kind of alkaline dye. It is widely used in the dyeing process of leather, paper and so on. In addition, crystal violet is also widely used in the pharmaceutical industry, reagent products and pharmaceutical intermediates. Its properties are shown in Table 1 [1-5]. With an increase in dosage, a large amount of crystal violet (CV) is discharged into wastewater, which can lead to obvious color changes in water bodies in terms of chromaticity. More

seriously, because it has carcinogenicity, mutagenicity and reproductive toxicity, it causes great harm to humans, animals and plants, and this harm may be long-term and potentially dangerous. Therefore, wastewater containing crystal violet must be treated to meet standards before it can be discharged [6-7]. During the treatment of wastewater containing crystal violet, crystal violet is not easily completely oxidized and degraded through microbial metabolism. This type of wastewater is considered refractory wastewater. This is because as a triphenylmethane-based compound, the aromatic ring structure within its molecular structure is difficult to decompose [8-9].

Table 1. Properties of crystal violet

name	Crystal violet
IUPAC name	4,4,4-Tris(dimethylamino)triphenylmethane
CAS number	603-48-5
Molecular structure	
Empirical formula	$C_{25}H_{30}N_3$
Molar weight	408 g/mol
LD50 (mouse)	96 mg/kg

At present, in the treatment of crystal violet-containing wastewater, most physicochemical methods, such as adsorption and precipitation, are combined with biological methods and other various methods [10-11]. For example, when using activated carbon as the adsorbent in the process of crystal violet wastewater treatment, although it has the advantages of good adsorption performance and a decolorization effect, the cost in the process of crystal violet-containing wastewater treatment is increased due to great difficulties in the regeneration and utilization of activated carbon, so the use of this method has great limitations. In addition, the more popular membrane separation technology relies on membrane holes that are easily blocked in the treatment of crystal violet-containing wastewater, requires a long pretreatment process and regular chemical cleaning, and facilitates the treatment of concentrate with great difficulty, which limits its application in the treatment of crystal violet-containing wastewater. Although some methods have good effects, they are difficult to popularize, such as supercritical water oxidation, which needs to be carried out under high temperature and high pressure. This not only increases the treatment cost but also necessitates the development of catalysts with high stability and high activity. Although these methods can effectively reduce the concentration of crystal violet and reduce the harm to the ecological environment and human health to a certain extent, various treatment methods have their own advantages and disadvantages. Therefore, exploring a method that can quickly and efficiently degrade crystal violet in water, especially the aromatic ring structure of crystal violet, is an important research topic for solving this kind of environmental pollution problem [12-13].

Among the treatment methods for various refractory wastewaters, the electrocatalytic oxidation method has the characteristics of safety, high efficiency and no secondary pollution. It also has the advantages of simple posttreatment, small floor area and convenient management. It is considered a clean treatment method, so it is widely studied and applied [14-15]. In the practical application of the treatment of wastewater produced from the printing and dyeing industries, it has been proven that electrochemical methods can quickly and effectively reduce the high COD index of water pollutants, basically meet the discharge requirements after treatment, and improve the biodegradability of wastewater, laying a foundation for further advanced treatment [16-17]. At present, there are many electrochemical methods for the treatment of refractory wastewater, mainly including electrocatalytic oxidation, electroflotation, electroflocculation, microelectrolysis, magnetic electrolysis and Fenton electrolysis [18]. PbO₂ electrodes are widely used in the fields involving the electrolytic preparation of organic matter and sewage treatment because of their low resistivity, stable chemical properties, good corrosion resistance, high current, excellent reversible charge–discharge performance and low cost [19-21]. In this study, crystal violet solution was degraded by electrocatalytic oxidation using an electrochemical method. A titanium-based lead dioxide nanoelectrode was prepared by electrodeposition with titanium metal as the substrate for the working electrode to degrade crystal violet by electrocatalytic oxidation. The effects of the initial concentration of crystal violet, current density, electrolyte concentration and pH value on the degradation of crystal violet were studied, the electrocatalytic degradation performance of the lead dioxide electrode with regard to crystal violet was explored, and the mechanism of the catalytic oxidative degradation of crystal violet was proposed. The mechanism was verified in an actual wastewater treatment process, which provides a theoretical basis and practical experience for the technology of treating crystal violet pollutants in the environment.

2. EXPERIMENT

2.1 Materials

In the experiment, crystal violet was purchased from Tianjin Dingshengxin Chemical Co., Ltd. Titanium plates were purchased from Tengxin Titanium Industry Co., Ltd. N-Butanol was purchased from Tianjin Kermel Chemical Reagent Co., Ltd. Stannous chloride was purchased from Tianjin Kaitong Chemical Reagent Co., Ltd. Antimony trichloride was purchased from Tianjin Kemio Chemical Reagent Co., Ltd. Anhydrous sodium sulfate was purchased from Vicote Chemical Products Trading Co., Ltd.

2.2 Preparation and characterization of the electrode

After preparing a 0.2 mol/L Pb(NO₃)₂ solution, a PbO₂/Ti electrode was prepared by electrodeposition in the solution. During the preparation of the electrode, the temperature was controlled at 25 °C, the pH was adjusted to 2.0±0.1 with 0.1 mol/L nitric acid, the current density was set to 30 mA/cm², and the electrodeposition time was controlled to 60±1 minutes. The pretreatment of the titanium substrate and the preparation of the SnO₂-Sb₂O₃/Ti interlayer were the same as in our previous

work. SnO₂-Sb₂O₃/Ti electrodes were used as the anodes, and a Pb plate was used as the cathode [22]. The electrode structure was analyzed by a D8 focus X-ray diffractometer (XRD) from AXS Co., Ltd. in Brooke, Germany, a G2 Pro scanning electron microscope (SEM) from Shanghai Funa Scientific Instrument Co., Ltd., and an electrochemical workstation from Shanghai ChenHua Co., Ltd. Using the f280 fluorescence spectrophotometer of Tianjin Gangdong Technology Development Co., Ltd., the excitation wavelength was 340 nm, and the recording range was 400 to 560 nm. With 0.8 mmol/L coumarin as the electrolyte and 0.01 mM H₂SO₄ as the fluorescent probe, the pH value was adjusted to 3.84. The samples were analyzed and measured at different current densities from 30 to 150 mA/cm².

2.3 Electrocatalytic oxidation performance of the lead dioxide electrode

During the experiment, analytical pure crystal violet reagent and pure water are used as solvents to prepare the experimental wastewater with corresponding concentrations. The experimental device is shown in Fig. 1. The electrode is prepared by an electrodeposition method. The anode is a titanium-based PbO₂ electrode, the cathode is a titanium plate electrode, and the electrolyte is a Na₂SO₄ solution with a corresponding concentration produced by using analytical pure anhydrous sodium sulfate. The experiment utilizes a DC power supply [23-25]. The effects of the conductive current density, solution pH, initial concentration of crystal violet and electrolyte Na₂SO₄ concentration on the performance of the electrode are investigated. In this experiment, UV-vis (MAPADA UV-18000PC-DS) spectrophotometry is used to analyze the concentration of the crystal violet solution. The maximum characteristic absorption peak wavelength of crystal violet in aqueous solution is 482 nm. According to the experimental requirements, the absorbance of the solution is measured at this wavelength at the corresponding time interval to obtain the concentration of crystal violet after degradation, the concentration change before and after the experiment is obtained, and then the degradation rate of crystal violet is calculated. See Formula 1 for the calculation method. Since the COD value can indirectly reflect the effect of pollutant degradation, a potassium dichromate method is also used to determine the COD value of the solution in the experimental process to evaluate the removal rate of crystal violet. The calculation method is shown in Formula 2. According to the calculation results, the purpose of determining the optimal process conditions for the degradation of crystal violet by the PbO₂/Ti electrode can be achieved [26]. The degradation mechanism and efficiency of the experimental device in CV-containing wastewater were determined by Shimadzu gas chromatography-mass spectrometry (GCMS-QP2020) with the same method as in our previous work [22].

$$\text{Removal rate} = \frac{\text{Initial CV concentration} - \text{CV concentration after treatment}}{\text{Initial CV concentration}} \quad \text{Formula 1}$$

$$\text{Removal rate} = \frac{\text{Initial wastewater COD concentration} - \text{COD concentration of treated wastewater}}{\text{Initial wastewater COD concentration}} \quad \text{Formula 2}$$

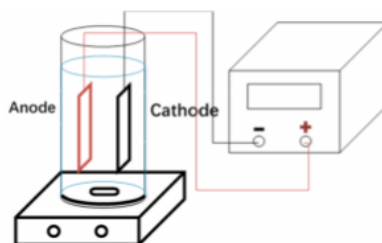
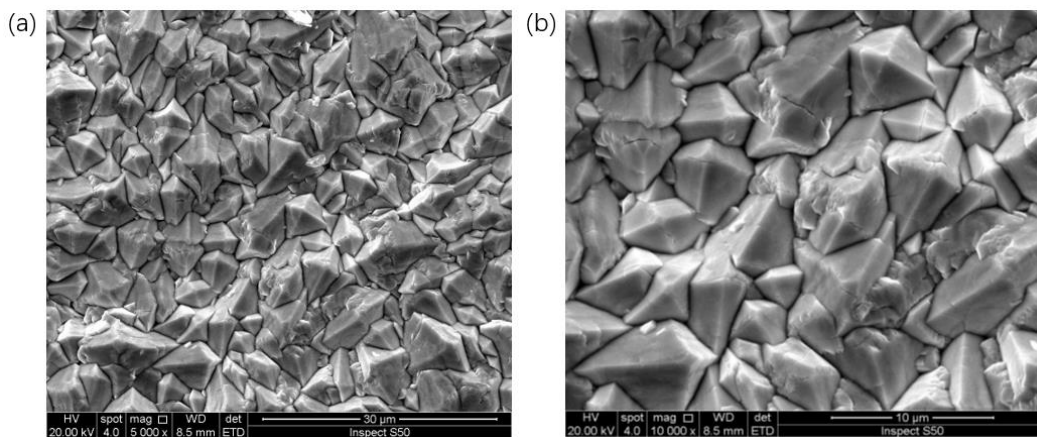


Figure 1. Schematic diagram of the experimental device for the electrocatalytic oxidation degradation of crystal violet solution.

3. RESULTS AND DISCUSSION

3.1 Characterization of the PbO_2/Ti electrode

Fig. 2(a) and Fig. 2(b) display the SEM images of the PbO_2/Ti electrode observed under an electron microscope with magnifications of 2000 and 5000 times, respectively. From the SEM images of the PbO_2/Ti electrode, it is obvious that the surface structure of the electrode presents a dense state as a whole, and the dense state distribution is very uniform. It can also be seen from Fig. 2(b) that the PbO_2/Ti electrode belongs to the cubic crystal system, which conforms to the β -structure of PbO_2 [27]. Fig. 2(c) shows the EDS spectrum of the PbO_2/Ti electrode. The highest peak observed in the figure belongs to the characteristic peak of lead. Through quantitative analysis, lead accounts for more than 90 wt% of the sample mass, which shows that lead is successfully loaded onto the titanium matrix and that the PbO_2/Ti electrode is successfully prepared [28]. Fig. 2(d) is the XRD diagram of the PbO_2/Ti electrode. It can be observed that there is a minimum near 75° and a maximum near 25° , which is characteristic of β - PbO_2 [29]. Fig. 2(d) shows the X-ray diffraction peak pattern of the PbO_2 electrode. In the XRD diagram, approximately 25° , 28° , 32° , 36° , 48° , 53° , 64° and 75° correspond to the (110), (111), (101), (200), (211), (220), (301) and (321) crystal planes of β - PbO_2 , respectively, which is consistent with the SEM results seen in Fig. 2 (b).



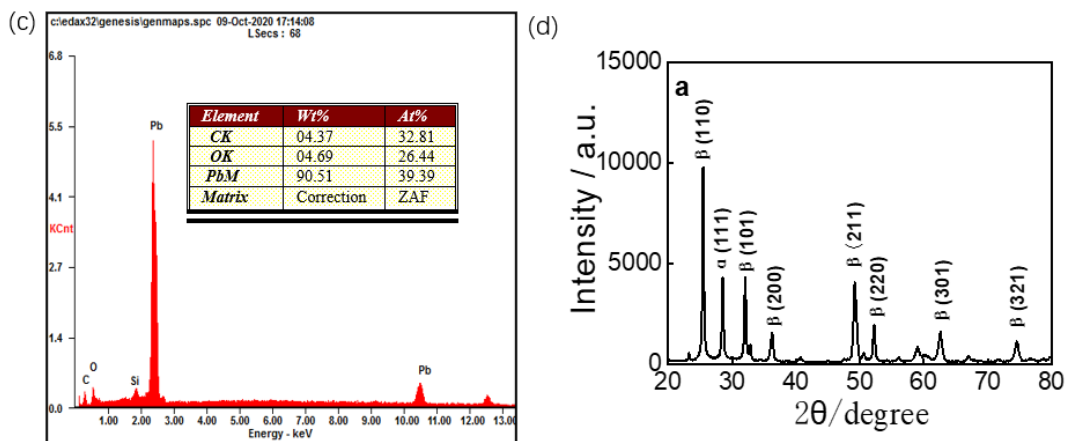


Figure 2. (a) PbO₂/Ti electrode surface (2000) ×; (b) PbO₂/Ti electrode surface (5000) ×; (c) EDS diagram of PbO₂/Ti electrode; (d) XRD of PbO₂/Ti electrode.

3.2 Electrochemical properties of the PbO₂/Ti composite electrode

The generation of electrode polarization inevitably simultaneously reduces the potential of the cathode and increases the potential of the anode. Fig. 3(a) shows the polarization curve of the lead dioxide electrode. It can be seen from the figure that the corresponding oxygen evolution potential is 1.58 V. Fig. 3(b) shows the fluorescence spectrum observed during the electrocatalytic oxidation of the PbO₂/Ti electrode. It can be seen from the figure that there is an obvious fluorescence intensity at 430 nm. With increasing reaction time, the fluorescence intensity increases greatly due to product accumulation. This shows that the concentration of ·OH radicals increases with increasing electrolytic reaction time, which shows that the lead dioxide electrode can produce hydroxyl radicals and has a good catalytic effect [30].

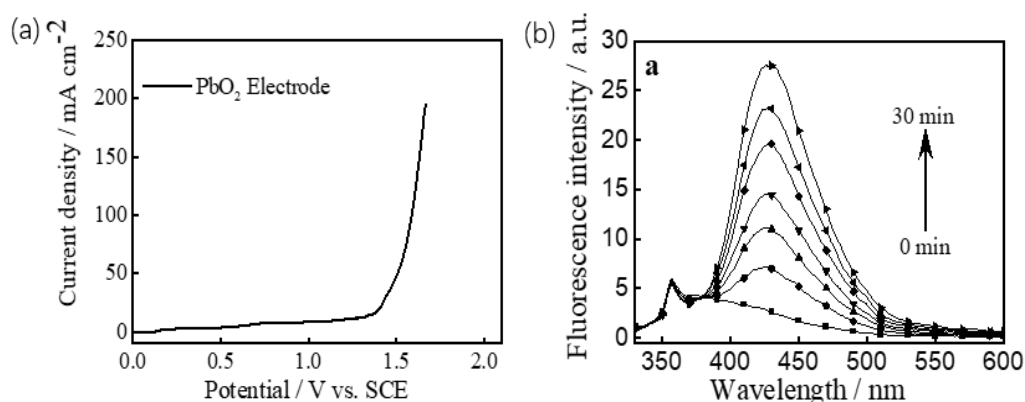


Figure 3. (a) Polarization curve of the PbO₂/Ti electrode at a scan rate of 10 mV/s in Na₂SO₄ solution. (b) Fluorescence spectrum observed during the electrocatalytic oxidation of the PbO₂/Ti electrode.

3.2.1 Initial concentration effect on the degradation of crystal violet

Fig. 4(a) shows the trend of the crystal violet removal rate within 180 minutes under the initial concentration of crystal violet at concentrations of 10, 20, 30, 40 and 50 mg/L. At the current density of 55 mA/cm^2 , the pH value is 4, and the electrolyte concentration of Na_2SO_4 is 0.2 mol/L . It can be seen from the figure that the removal rate of crystal violet with different concentrations shows an increasing trend with increasing reaction time, which shows that the electrode has a good degradation effect on crystal violet in a short time. The removal rate of crystal violet increases with decreasing crystal violet concentration because the electrocatalytic degradation process of the hydroxyl radicals occurs on the anode surface, the concentration of pollutants increases, and the electrolytic process is limited by diffusion [31]. At a lower concentration of crystal violet, the oxidation rate of crystal violet and the formation rate of its decomposition products are higher than the mass transfer rate of crystal violet from the solution. At this time, crystal violet is rapidly oxidized on the electrode surface, and most of the intermediate products produced in the oxidation process are rapidly decomposed into CO_2 and H_2O . Therefore, the COD removal rate is high at this time [32]. When the concentration of crystal violet increases, the removal rate of crystal violet is low. This is because with the increase in the initial concentration of crystal violet, more pollutants to be degraded are gathered near the electrode surface, and the increasing concentration of intermediate products produced during the electrochemical degradation process have a competitive relationship with hydroxyl radicals in the process of the reaction. As a result, crystal violet cannot be rapidly degraded into the final product, resulting in a reduction in the removal rate of crystal violet [33]. In addition, we can also see that at a low concentration of crystal violet, the removal rate of COD almost reaches a stable state after 90 minutes, and the removal rate does not increase significantly with increasing time. This is because at a low concentration, crystal violet reacts effectively with hydroxyl radicals and rapidly decomposes into intermediate products, which are difficult to degrade by the electrode and cannot be completely oxidized to water and carbon dioxide. Fig. 4(b) shows that the degradation rate of crystal violet increases exponentially, which is consistent with the kinetics of a first-order reaction [34]. See Table 2 for the kinetic data.

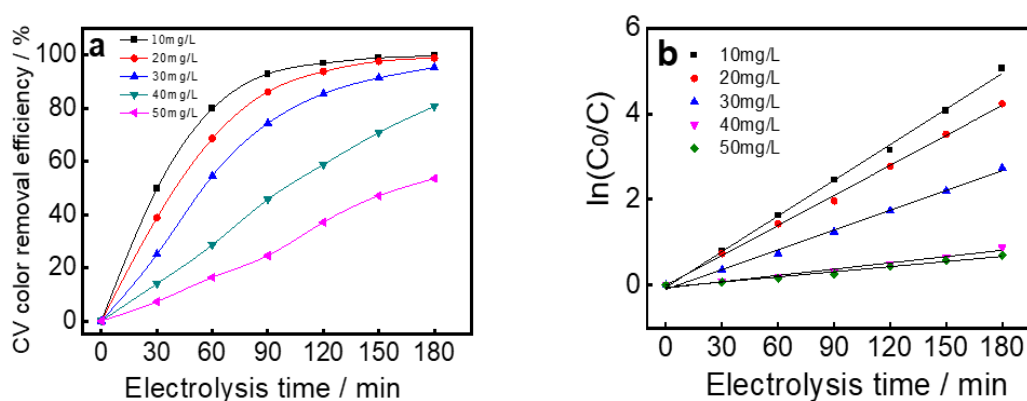


Figure 4. Effect of the initial concentration of crystal violet on the degradation reaction.

3.2.2 Current density effect on the degradation of crystal violet

Current density is an important energy consumption index for the treatment of wastewater containing crystal violet and determines the degradation rate of crystal violet on the electrode surface. As shown in Fig. 5(a), the crystal violet removal rate increases sharply with increasing current density. When the current density increases from 15 mA/cm² to 55 mA/cm², the pH value is 4, the crystal violet concentration is 50 mg/L, and the electrolyte concentration of Na₂SO₄ is 0.2 mol/L. Moreover, the degradation time is 180 minutes, and the removal rate of crystal violet increases from 57% to 99%. This is because the generation rate of hydroxyl radicals is positively correlated with the current density. With increasing current density, the number of hydroxyl radicals on the anode surface increases greatly. Therefore, in the process of the electrocatalytic degradation of crystal violet by the electrode, with increasing current density, more hydroxyl radicals are generated so that more charges are directly transferred from crystal violet to the anode, which promotes the degradation reaction and increases the removal rate of crystal violet [35]. Fig. 5(b) shows that (C_0/C_t) has a good linear relationship with the degradation time, indicating that the electrocatalytic oxidation degradation process of crystal violet corresponds to a first-order reaction kinetic process and belongs to a quasi-first-order reaction. See Table 2 for the kinetic data. The larger the slope of the kinetic curve of the electrode electrocatalytic degradation process is, the faster the rate of electrocatalytic degradation of crystal violet and the better the degradation effect.

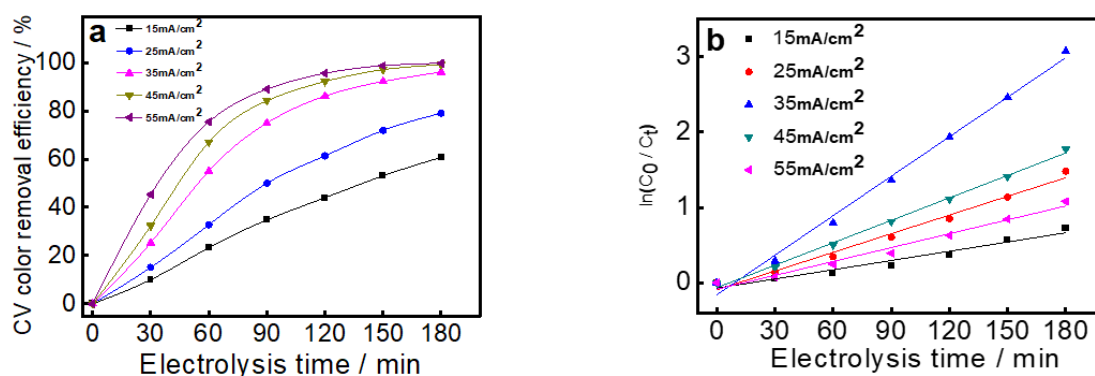


Figure 5. (a) Effect of current density on the degradation of crystal violet. (b) Kinetic curve.

3.2.3 Effect of pH on crystal violet degradation

The effect of the initial solution pH value (2.0-10.0) on the degradation rate of crystal violet is analyzed, as shown in Fig. 6(a). At a current density of 55 mA/cm², the crystal violet concentration is 50 mg/L, and the electrolyte concentration of Na₂SO₄ is 0.2 mol/L. As shown in Fig. 6(a), when the pH is 2, the maximum degradation rate of crystal violet is ($k=0.0498 \text{ min}^{-1}$). When the pH is 4, the degradation rate of crystal violet decreases slightly but still has a good electrolytic effect. When the pH is 6, the degradation rate of crystal violet decreases significantly. With a further increase in the pH value, the degradation rate decreases significantly. From the mechanism analysis, this is because the generation

rate of $\cdot\text{OH}$ is directly proportional to the acid intensity; that is, when the pH value needs to be controlled at a lower level, more $\cdot\text{OH}$ can be generated at the same time to better participate in the degradation reaction and improve the removal rate of crystal violet. However, under strong acid conditions, serious corrosion of the PbO_2/Ti electrode occurs, which not only reduces the service life of the PbO_2/Ti electrode and is not conducive to long-term and efficient degradation experiments but also produces a certain number of corrosion products as the corrosion reaction progresses, resulting in secondary pollution. The degradation of crystal violet at different initial pH values, the service efficiency and service life of the electrode, as well as the cleaning of subsequent corrosion products and possible safety problems must be comprehensively considered. Finally, the initial pH value of the solution is 4, which is the best condition for the degradation of crystal violet [36]. As shown in Fig. 6 (b), (C_0/C_t) shows a good linear relationship with the electrocatalytic oxidation time, which shows that the electrocatalytic oxidation degradation process of crystal violet also conforms to a first-order reaction kinetic equation and belongs to the quasi-first-order reaction. See Table 2 for the kinetic reaction data. In the process of electrode electrocatalytic degradation, the lower the pH value is, the greater the slope of the first-order reaction kinetics curve. At this time, the faster the electrocatalytic degradation rate of crystal violet, the better the degradation effect.

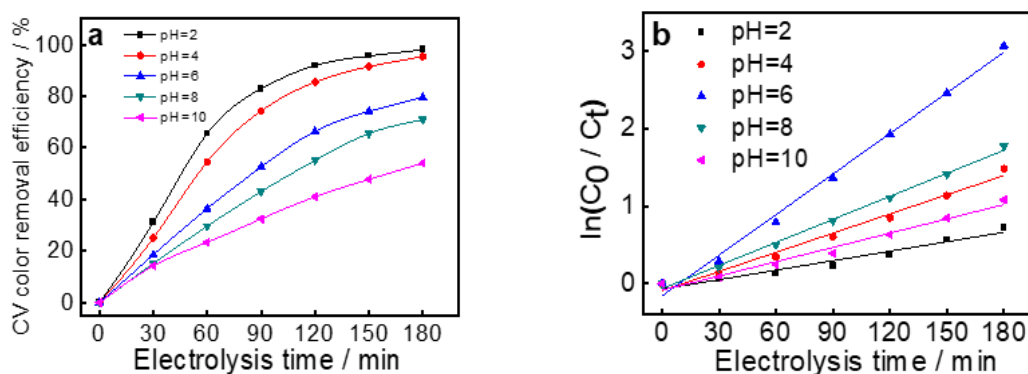


Figure 6. (a) Effect of pH on the degradation of crystal violet. (b) Kinetic curve.

3.2.4 Electrolyte concentration effect on the degradation of crystal violet

Due to the low conductivity of the crystal violet solution, to increase the conductivity of wastewater, the electrolyte Na_2SO_4 needs to be added in the process of electrochemical catalytic degradation. To determine the best dosage concentration, a single-factor variable experiment of the Na_2SO_4 electrolyte concentration was carried out. The crystal violet solution was placed in the electrocatalytic oxidation experimental device, the pH value was adjusted to 4.0 ± 0.1 , and the current density was 50 mA/cm^2 . The degradation reaction was carried out under DC for 180 minutes. The effect of electrolyte concentration on the degradation of crystal violet was studied. In the experiment, the concentration of the electrolyte Na_2SO_4 was set to 0.1 mol/L , 0.2 mol/L , 0.3 mol/L and 0.4 mol/L . The experimental results are shown in Fig. 7 (a) below. It can be seen from the figure that when the electrolyte Na_2SO_4 concentration was constant, the experimental reaction time increased, the crystal violet removal

rate continued to rise, and the degradation effect was very obvious. It can also be seen from the experimental data that when the electrolyte concentration of Na₂SO₄ was 0.2 mol/L, the removal rate of crystal violet reached the highest level, and the degradation rate of crystal violet decreased with the continuous increase in the electrolyte concentration of Na₂SO₄. This is because the electrolyte Na₂SO₄ plays a role in the decomposition process and increases the conductivity of the solution. With the continuation of the decomposition reaction, the amount of electrolyte produced increases the conductivity of the electrolytic system, and the interaction between point ions in the system will also increase. Therefore, the selection of the best electrolyte concentration involves the comprehensive consideration of the protection of various parts of the degradation system and the degradation of crystal violet at different concentrations, and the concentration of electrolyte Na₂SO₄ was determined to be 0.2 mol/L as the best condition for the degradation of crystal violet [37]. Fig. 7 (b) shows that the effect of the electrolyte concentration on the CV degradation rate also conforms to a first-order reaction kinetic equation, which is a quasi-first-order reaction. See Table 2 for the kinetic reaction data.

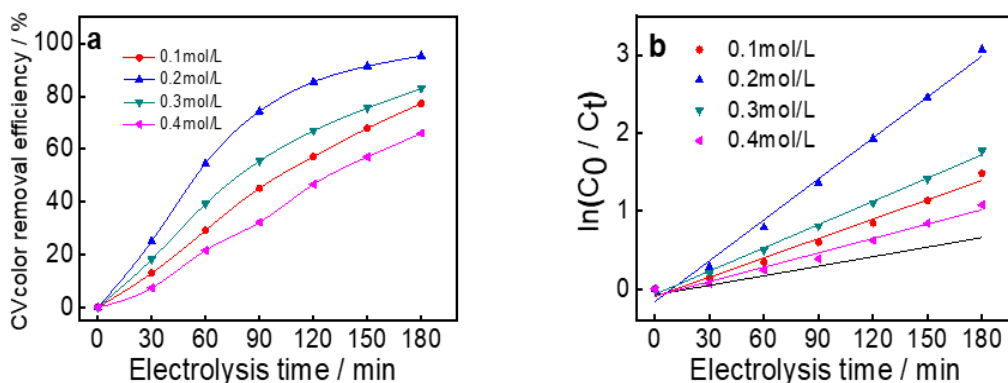


Figure 7. (a) Effect of electrolyte concentration on the degradation of crystal violet. (b) Kinetic curve.

Table 2. Corresponding kinetic data of the effects of experimental variables on CV degradation rate

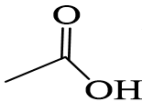
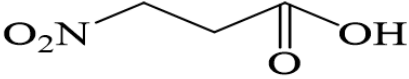
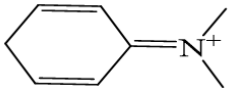
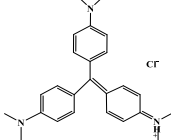
influence factor	numerical value	rate constant K (min ⁻¹)	correlation coefficient R ²
Initial concentration of CV (mg/L)	10	0.0608	0.9973
	20	0.0483	0.9941
	30	0.0325	0.9943
	40	0.0163	0.9815
	50	0.0080	0.9863
current density (mA/cm ²)	15	0.0098	0.9969
	25	0.0162	0.9947
	35	0.0325	0.9943
	45	0.0432	0.994
	55	0.0504	0.9981
Initial pH	2	0.0315	0.9968
	4	0.0244	0.9943
	6	0.0325	0.9943

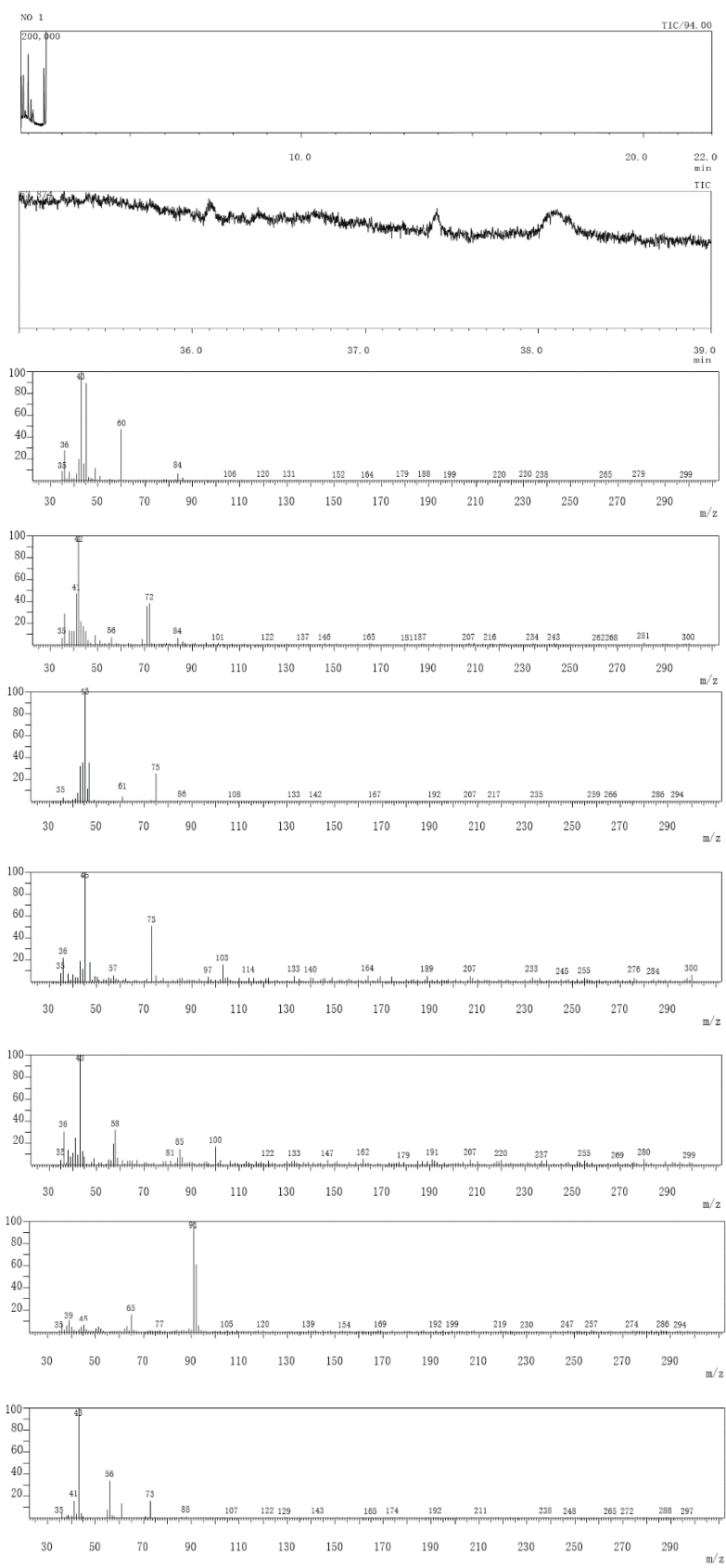
	8	0.0102	0.9971
	10	0.0065	0.9995
Electrolyte concentration	0.1	0.0151	0.9892
(Na ₂ SO ₄) (mol/L)	0.2	0.0325	0.9943
	0.3	0.0189	0.997
	0.4	0.011	0.9834

3.3 Mechanism analysis

Through the mass spectrum analysis of the degradation products in each experiment, after 180 minutes of reaction, six degradation products are mainly detected, as shown in Table 3, and Fig. 8 shows the corresponding mass spectra. It can be seen from the table that crystal violet reacts with the hydroxyl radicals generated by the lead dioxide electrode and degrades into a nitrobenzene structure, as shown in the entries A5 and A6 in the table. Under the action of the hydroxyl radicals, the benzene ring continues to open and decomposes into carboxylic acid and other small molecular compounds, such as those represented by entries A1 ~ A4 in Table 3, and finally oxidizes into CO₂ and H₂O under the further action of the hydroxyl radicals [38-39].

Table 3. Intermediate products after 180 minutes of degradation by GC-MS

No.	Retention time (min)	Structural formula
A1	1.184	
A2	2.470	
A3	4.020	
A4	5.106	
A5	10.851	
A6	14.843	
A7	37.410	



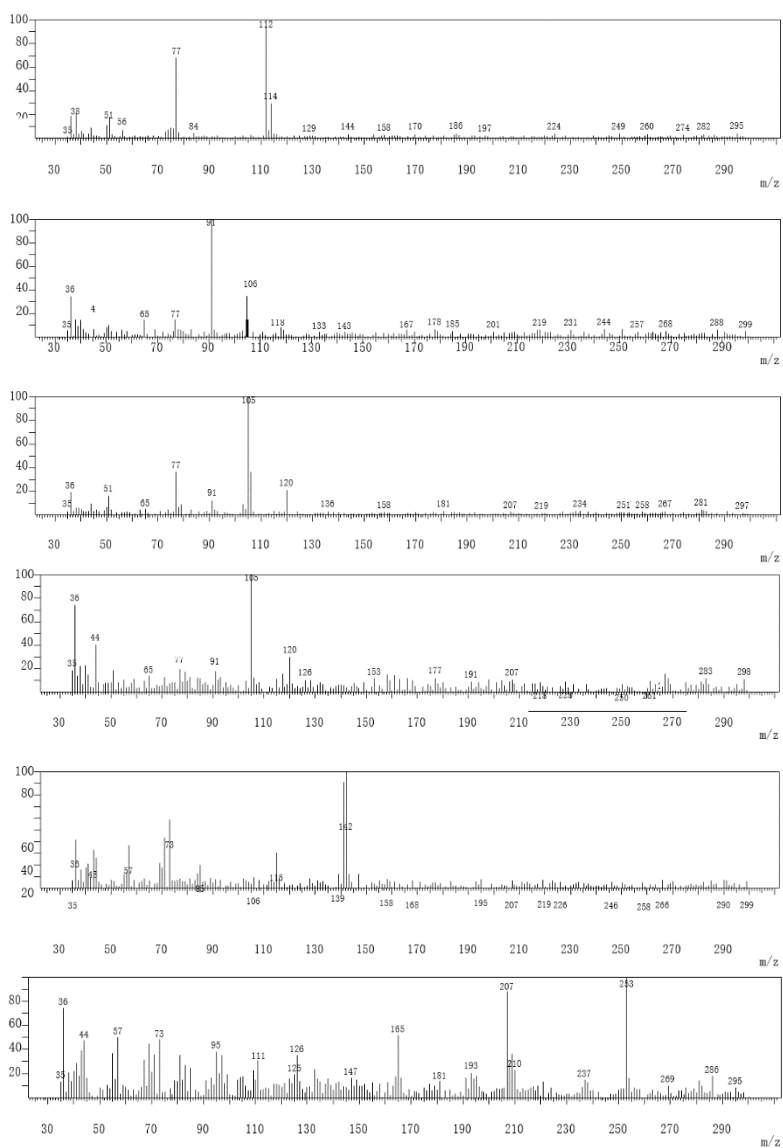


Figure 8. Mass spectra.

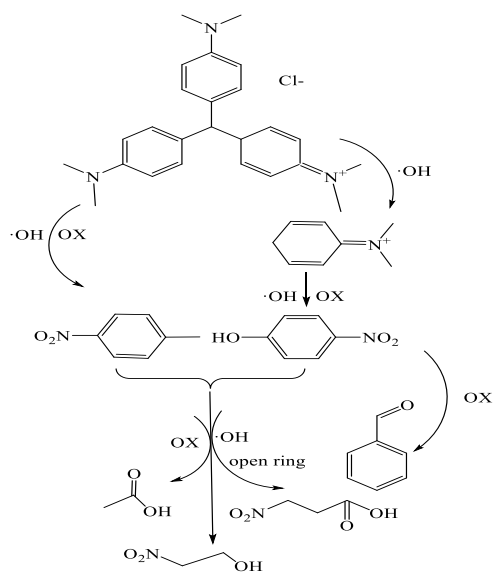


Figure 9. Crystal violet degradation mechanism

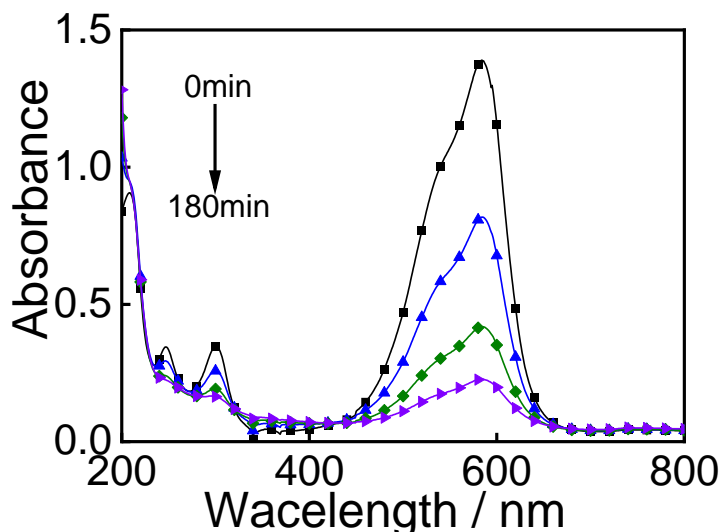


Figure 10. Ultraviolet–visible absorption spectrum of degraded crystal violet

Through the above analysis, the degradation mechanism of crystal violet can be inferred, and the degradation mechanism is shown in Fig. 9. The UV–Vis absorption spectrum of crystal violet degraded by the electrode is shown in Fig. 10. From the figure, it can be seen that the absorption peak of crystal violet at 590 nm decreases significantly, which further indicates that crystal violet has significantly degraded within 180 minutes.

3.4 CV degradation in the real samples

The wastewater used in the following experiments comes from a dye factory. See Fig. 11. for the chromatograms of the wastewater pollutants. The main component of the wastewater is crystal violet. The COD value of the wastewater for different experiments fluctuates in the range of 600–650 mg/L. Under a current density of 55 mA/cm², pH value of 4±0.1 and electrolyte concentration of Na₂SO₄ of 0.2 mol/l, the highest COD removal rate is close to 89% after electrolytic treatment for 6 h, and the remaining COD values are lower than the national discharge standard of 120 mg/L. The experimental results are shown in Fig. 10. The treatment of actual wastewater further shows that the catalytic degradation effect of the electrode on crystal violet in wastewater can basically meet the discharge requirements. The biodegradability of the small molecular organics produced by degradation must be better than crystal violet, which provides better conditions for subsequent biological treatment and advanced treatment.

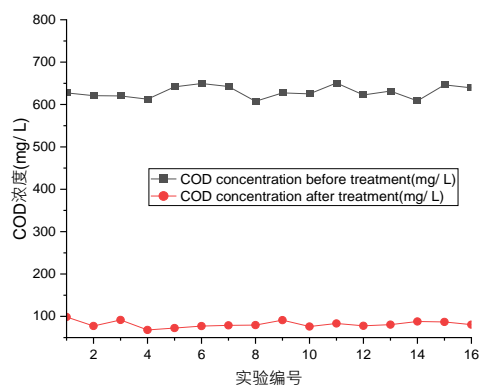
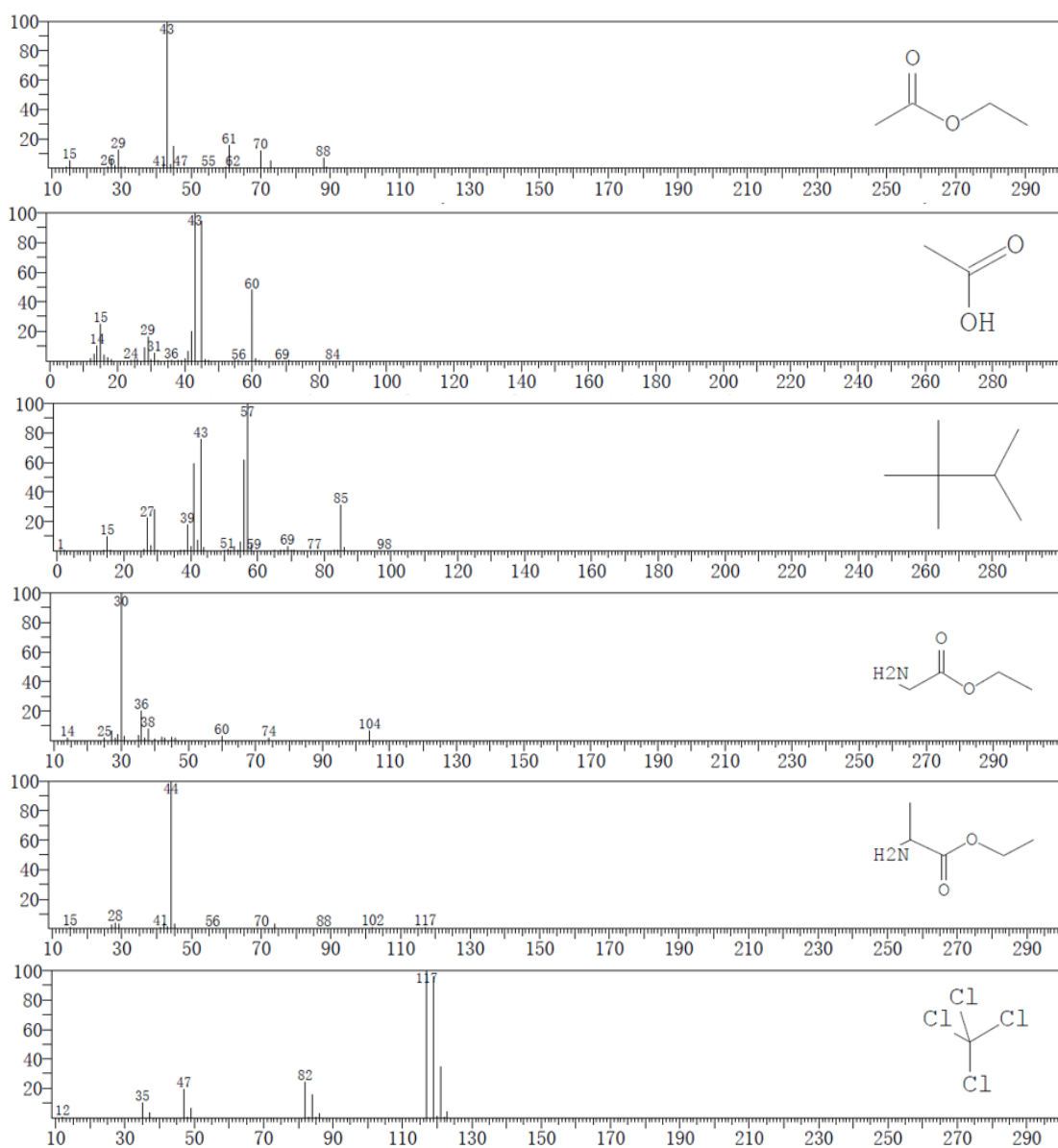


Figure 10. Trend chart of the wastewater experiment.



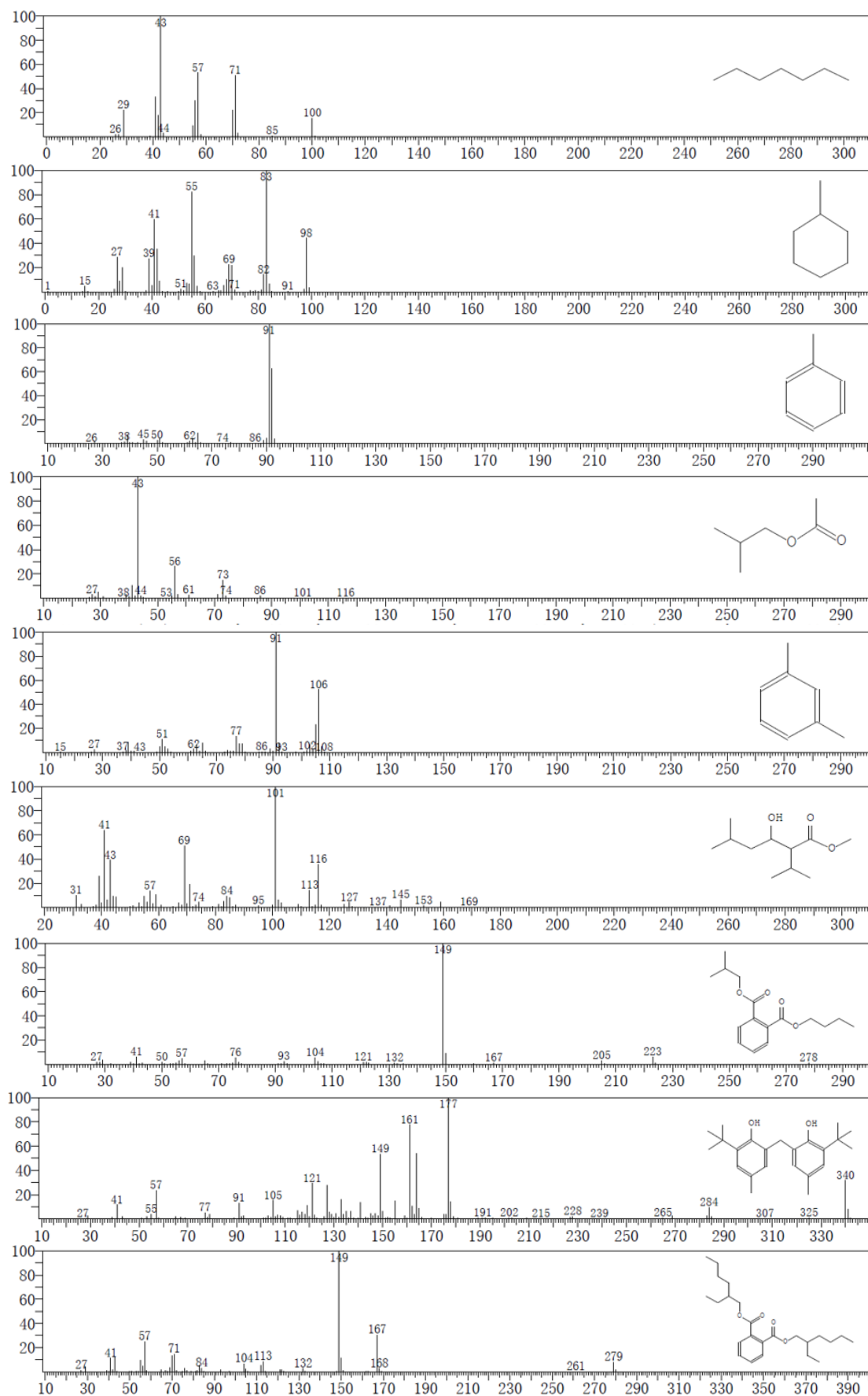


Figure 11. Chromatograms of the wastewater pollutants.

4. CONCLUSION

The PbO₂ electrode has a good degradation effect on crystal violet. According to the experiment, the higher the current density is, the better the degradation effect. Moreover, an acidic pH value is the most favorable for degradation, and the degradation effect is the best when the electrolyte concentration of Na₂SO₄ is controlled to 0.2 mol/L. According to the analysis of the experimental results, the final optimal conditions are as follows: a current density of 55 mA/cm², a pH value of 4±0.1, and an electrolyte concentration of Na₂SO₄ of 0.2 mol/L. On this basis, experiments were carried out on wastewater containing crystal violet. The degradation effect of the electrode on crystal violet was further confirmed from 16 groups of experimental data, which showed that this experimental device can produce treated wastewater that basically meets the discharge requirements of wastewater containing crystal violet in a short time.

ACKNOWLEDGMENTS

The project was supported by the Scientific Research Program of Tianjin Education Commission (No. 2021KJ090). This project was supported by the school enterprise collaborative innovation project of Tianjin Vocational University (XQXT202011022).

DECLARATION OF INTERESTS

The authors declare that they have no known competing financial interests or personal relationships that could have appeared to influence the work reported in this paper.

References

1. P. Sharma, N. Sohal and B. Maity, *RSC Adv.*, 11(2021)10912.
2. P.A. Ajibade and A.E. Oluwalana, *Nanomaterials-Basel*, 11(2021):2000.
3. V. Torres-Zúiga and O.G. Morales-Saavedra, *Mater. Chem. Phys.*, 133 (2012)1071.
4. M.F.H. Al-Kadhemy, *Res. Rev. Polym.*, 4(2013):45.
5. H. Ghanadan, M. Hoseini, A. Sazgarnia and S. Sharifi, *J. Electron. Mater.*, 48(2019) 7417.
6. A.M. Hidalgo, G. León, M. Gómez, M.D. Murcia and J.A. Macario, *Membranes*, 10(2020)408.
7. A. Mittal, J. Mittal, A. Malviya, D. Kaur and V.K. Gupta, *J. Colloid Interface Sci.*, 343(2010)463.
8. C.Y. Chen, J.T. Kuo, H.A. Yang and Y.C. Chung, *Chemosphere*, 92(2013)695.
9. H.R. Arias, P. Bhumireddy and C. Bouzat, *Int. J. Biochem. Cell Biol.*, 38(2006):1254.
10. K. Belkassa, M. Khelifa, I. Batonneau-Gener, K. Marouf-Khelifa and A. Khelifa, *J. Hazard. Mater.*, 415(2021)125656.
11. Y. Stolze, F. Eikmeyer, D. Wibberg, G. Brandis, C. Karsten, I. Krahn, S. Schneiker-Bekel, P. Viehover, A. Barsch and M. Keck, *Microbiology*, 158(2012)2060.
12. G. Tomazetto, S. Hahnke, I. Maus, D. Wibberg, A. Pühler, A. Schlüter and M. Klocke, *J. Biotechnol.*, 192(2014)59.
13. Y. Xiang, L. Xin, J. Hu, C. Li and X.H. Wei, *Crystals*, 11 (2021)47.
14. A. Maljaei, M. Arami and N.M. Mahmoodi, *Desalination*, 249(2009)1074.
15. H.J. Kumari, P. Krishnamoorthy, T.K. Arumugam, S. Radhakrishnan and D. Vasudevan, *Int. J. Biol. Macromol.*, 96(2017)324.
16. S. Mahesh, G. Kumar and P. Agrawal, *J. Environ. Biol.*, 31(2010)277.
17. K.S. Vipran, *Res. J. Chem. Environ.*, 22(2018)16.
18. D. Nguyen, H. Quang, H.N. Xuan and P.N. Tan, *RSC Adv.*, 11(2021)27443.
19. Z. Falaki and H. Bashiri, *J. Iran. Chem. Soc.*, 18(2021)2689.

20. T. Yun, C. Pengzuo, Z. Mengxing, Z. Tianpei, Z. Lidong, C. Wangsheng, W. Changzheng and X. Yi, *ACS Catal.*, 8(2018)1.
21. A. Safavi, R. Ahmadi, F.A. Mahyari and M. Tohidi, *Sens. Actuators, B.*, 207(2015)668.
22. Y. Naichuan, W. Jingyu, G. Zhensheng, S. Hailong, G. Yong, Z. Jun, L. Xi, N. Pan and H. Enshan, *Chemosphere*, 289(2022)133014
23. Y. Yingwu, Z. Manman, Z. Chunmei and W. Xiao, *J. Electrochem. Soc.*, 160(2013)553.
24. V. Baglio, A.D. Blasi, T. Denaro, V. Antonucci and L.G. Arriaga, *J. New Mater. Electrochem. Syst.*, 11(2008)105.
25. M. Bastaninejad, A.A. Elmustafa, E. Forman, S. Covert and P. Williams, *J. Vac. Sci. Technol.*, 33(2015)041401.
26. M. Hori, K. Nagasaka, M. Miyayama, G. Trunfio and E. Traversa, *Key Eng. Mater.*, 2006, 301(2006)155.
27. J. Li, M. Guo, Y. Shao, H. Yu and K. Ni, *ACS Omega*, 6(2021)5436
28. Y. Quan, M. Li, X. Shungen, Z. Dongxing and S. Lining, *Nanomaterials*, 11(2021)1290.
29. M. Li and Y. Li, *JOM*, 72 (2020)3806.
30. Z. Feng, Q. Tian, Q. Yang, Y. Zhou and G. Zhao, *Appl. Catal., B.*, 286(2021) 119908.
31. L.R. Aveiro, A.G.M. da Silva, E.G. Candido, E.C. Paz, V.S. Pinheiro, L.S. Parreira, F.M. Souza, V.S. Antonin, P.H.C. Camargo and M.C. dos Santos, *Electrocatalysis*, 11(2020) 268.
32. Y. Tang and C. Kong, *Mater. Chem. Phys.*, 135 (2012) 1108.
33. L.S. Andrade, L. Ruotolo, R.C. Rocha-Filho, N. Bocchi, S.R. Biaggio, J. Iniesta, V. García-García and V. Montiel, *Chemosphere*, 66(2007) 2035.
34. T.C. Loureno, M. Ebadi, D. Brandell, J. Silva and L.T. Costa, *J. Phys. Chem. B.*, 124(2020) 9648.
35. J. Li, D. Yan, W. zhang, J. Pu, B. Chi and L Jian, *Electrochim. Acta.*, 255 (2017) 31.
36. Q. Zhou, X. Zhou, R. Zheng, Z. Liu and J. Wang, *Sci. Total Environ.*, 806 (2022) 150088.
37. J. Ping, S. Rauf, Z. Tayyab, R. Wang, H. Xiao, L. Xu, S. Liang, Q. Huang and C. Yang, *Ceram. Int.*, 47(2020) 7898.
38. M. Panizza and G. Cerisola. *Chem. Rev.*, 109(2009) 6541.
39. G. Jing, Y. Junjuan, L. Youzhi, Z. Jiacheng and G. Zhiyuan. *Water Sci. Technol.*, 76(2017) 662.

© 2022 The Authors. Published by ESG (www.electrochemsci.org). This article is an open access article distributed under the terms and conditions of the Creative Commons Attribution license (<http://creativecommons.org/licenses/by/4.0/>).